Photocatalysis

International Edition: DOI: 10.1002/anie.201504135
German Edition: DOI: 10.1002/ange.201504135

Direct Imaging of Highly Anisotropic Photogenerated Charge Separations on Different Facets of a Single $BiVO_4$ Photocatalyst**

*Jian Zhu, Fengtao Fan, Ruotian Chen, Hongyu An, Zhaochi Feng, and Can Li**

Abstract: *Spatially resolved surface photovoltage spectroscopy (SRSPS) was employed to obtain direct evidence for highly anisotropic photogenerated charge separation on different facets of a single $BiVO_4$ photocatalyst. Through the controlled synthesis of a single crystal with preferentially exposed {010} facets, highly anisotropic photogenerated hole transfer to the {011} facet of single $BiVO_4$ crystals was observed. The surface photovoltage signal intensity on the {011} facet was 70 times stronger than that on the {010} facets. The influence of the built-in electric field in the space charge region of different facets on the anisotropic photoinduced charge transfer in a single semiconductor crystal is revealed.*

Photoinduced charge separation on the nano- to micrometer scale, with varying lifetimes, constitutes the key component of solar energy conversion devices.[1,2] Advancing these devices towards high light-to-energy conversion efficiencies requires an understanding of the photoinduced charge-transfer process and spatial separation at the nanoscale.[3–5] In recent years, the engineering of semiconductor-based photocatalysts with controlled morphology and preferentially exposed facets has proved an efficient way of improving photocatalytic activity.[6–11] In experiments with fluorescent and chemical probe molecules, it was found that probe molecules are selectively reduced or oxidized on certain facets of single TiO_2 crystals.[12,13] It was also found that reduction and oxidation cocatalysts can be selectively deposited on different facets of $BiVO_4$ crystals. Moreover, the resulting catalysts show much higher photocatalytic activity than those with cocatalysts randomly deposited on $BiVO_4$.[14] Therefore, it is proposed that preferred migration of photogenerated holes and electrons to specific crystal facets can lead to charge separation and result in higher photocatalytic activity.

However, facet-specific charge transfer may not be the sole cause of the improved photocatalytic activity. Using aqueous-phase atomic force microscopy (AFM), Mul et al. showed that the photodeposition of Pt nanoparticles on platelike WO_3 crystals occurs preferentially on the small, subordinate facets with intrinsic surface charges rather than photogenerated charges.[15] Obviously, despite these efforts to understand the role different facets play in photocatalysis, the intrinsic causes that lead to the different chemical/physical properties of different active sites/facets are quite ambiguous. To date, no direct evidence for anisotropic photoinduced charge transfer on the surface of these semiconductor single crystals has been reported. Here, we report the application of spatially resolved surface photovoltage spectroscopy (SRSPS) to obtain direct evidence of highly anisotropic photogenerated charge separation on different facets of a single $BiVO_4$ photocatalyst. Highly anisotropic photoinduced hole distribution is observed in single $BiVO_4$ crystals with preferentially exposed {010} facets, and the surface photovoltage (SPV) signal intensity on the {011} facet is 70 times stronger than that on the {010} facet.

Figure 1 a,b show SEM images of the single $BiVO_4$ crystal growth on fluorine-doped tin oxide (FTO) substrates synthesized with different preferential ramp rates of 2.25 and 1.50 $K\,min^{-1}$ as described in Figure S1 in the Supporting Information). As shown in the SEM images, each sample of $BiVO_4$ is crystallized in a highly isolated manner such that all crystals have nearly the same size and morphology. All the particles exhibit a truncated tetragonal bipyramid shape between the top and side facets. The slower ramp rate of 1.50 $K\,min^{-1}$ results in crystals approximately 8 μm in size with a flatter morphology, whereas 2.25 $K\,min^{-1}$ ramp rate

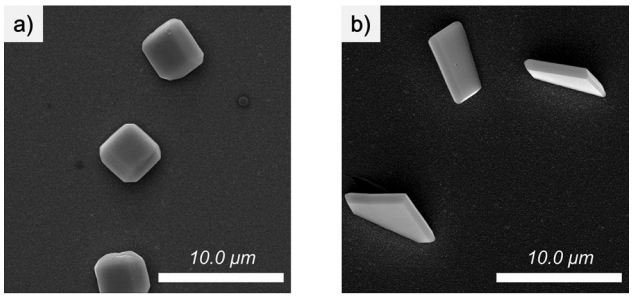

Figure 1. a, b) SEM images of single m-$BiVO_4$ crystals with different morphologies synthesized on FTO substrate. The morphology was altered by changing the ramp rates during hydrothermal synthesis from 298 K to 433 K. The m-$BiVO_4$ crystal in (a) and (b) are denoted BV01 and BV02, respectively.

[*] J. Zhu,[+] F. Fan,[+] R. Chen, H. An, Prof. Z. Feng, Prof. C. Li
State Key Laboratory of Catalysis, *i*ChEM, Dalian Institute of Chemical Physics, Chinese Academy of Sciences, Dalian National Laboratory for Clean Energy
Zhongshan Road 457, Dalian 116023 (China)
E-mail: canli@dicp.ac.cn
J. Zhu,[+] R. Chen, H. An
Graduate University of Chinese Academy of Sciences
Beijing 100049 (China Department)
[+] These authors contributed equally to this work.

[**] This work was financially supported by the 973 National Basic Research Programme of the Ministry of Science and Technology (Grant 2014CB239403), and the Key Research Program of the Chinese Academy of Sciences. We thank Dayong Fan and Xiuli Wang at DICP for performing the fluorescence spectroscopy experiment and Mingrun Li at DICP for performing the HRTEM experiment.
Supporting information for this article is available on the WWW under http://dx.doi.org/10.1002/anie.201504135.

results in crystals of approximately 5 μm. For brevity, crystals synthesized with ramp rates of 2.25 and 1.50 K min^{-1} are noted as BV01 and BV02, respectively. These crystals were further examined by Raman spectroscopy and HRTEM as shown in Figure S1. The results suggested that these crystals are highly crystallized monoclinic bismuth vanadate crystals with the top facet along {010} and the side facets along {110} and {011}.[16]

Kelvin probe force microscopy (KPFM) enables the study of the real surface of a semiconductor photocatalyst because it can operate at ambient pressure, temperature and humidity.[5,17–20] Figure 2 a,b show the topology and KPFM images of a single BV01 crystal. Surprisingly, the surface potential images of BV01 show potential diversity within one single crystal. As the KPFM image provides the contact potential difference (CPD) between the tip and the sample, the fact that the {010} facet appears darker on the color scale indicates that this facet has a more negative surface potential. In contrast, the brighter images of the {011} facets indicate that this facet has a more positive surface potential. Hudlet et al. demonstrated that, for a semiconductor surface, the measured CPD is related to the surface potential, which differs from the bulk work function of the semiconductor materials, due to the space charge region (SCR) near the semiconductor surface.[17] Thus, the different surface potentials of the two facets indicate that the two facets have different SCRs beneath the surfaces, although they share the same bulk Fermi levels. Upon irradiation with UV-LED, the KPFM image of $BiVO_4$ becomes brighter indicating increased surface potentials (Figure 2 c,d). The changes in surface potential clearly reflect that the charge balance in the SCRs beneath the two facets undergoes a significant change. The increased surface potentials suggest that the two facets have an upward band bending in the SCRs. Upon light excitation, photogenerated holes will be pulled out to the surface of a semiconductor, and the electron will flow into the SCRs beneath the facets. The redistributed charges lead to the potential increase across the SCR and hence the surface potentials.

According to the KPFM results, the surface potentials of the {011} and {010} facets differ from each other. However, it is interesting to note that, although the surface potential is restored to its original state after cutting off the excitation light, it takes at least 1 min to reach the previous dark state, as shown in Figure 2 e. Figure 2 f shows steady-state spatially resolved SPV spectra of the {010} and {011} facets and shows that the ΔCPD decreases slightly with decreased photoexcitation energy. Nonetheless, no significant decreases are observed around the band gap at 2.4 eV.

It has been proposed that the time required to reach the steady-state distribution depends on the thermal cross-sections and varies over many orders of magnitude.[20] Based on whether the charge in the surface states follows the chopped illumination, Bardeen and Brattain classified the SPV signal into fast and slow states.[20] Recently, Stutzmann et al. assigned the slow states to localized defect states close to the semiconductor surface.[21] Obviously, the trapping or recombination of the photogenerated charges within these unwanted defects will not take part in the photocatalytic

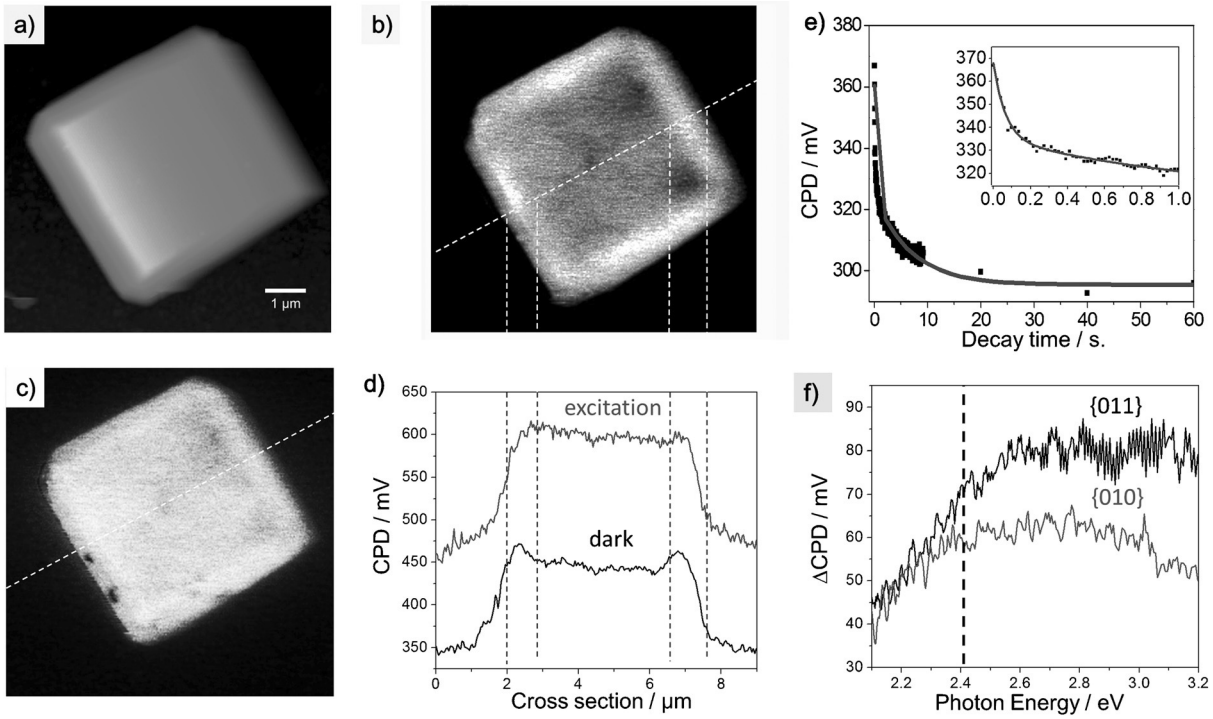

Figure 2. a–c) Topography and KPFM images of single $BiVO_4$ crystals on FTO substrates in the dark (b) and under irradiation with a UV-LED (c). d) Cross-sections of the surface potential images in (b) and (c), respectively. The brighter area indicates lower surface work function and higher surface potential. e) Plot of the surface potential as a function of decay time after cutting off the excitation light (450 nm). Insert: decay of surface potential within 1 s. The solid line is a guide the eye without mathematical fitting. f) Steady-state SPV spectroscopy of the {010} and {011} facets. The spectra were obtained by plotting ΔCPD (subtracting dark CPD from photoexcited CPD) as a function of the excitation photon energy.

surface reactions with millisecond time constant.[21] For the present case, our results indicate that the decay of the CPD undergoes at least two processes, one on hundred millisecond scale and another on minute scale.

A powerful technique to extract this information is to measure SPV with chopped light, denoted as transient SPV. By using modulated light and transient signals acquired by a lock-in amplifier, the slow component can be filtered to isolate the fast component in the SPV spectra.[22] Moreover, the electronic states upon illumination can be well resolved with tunable wavelength. Thus, by combining the KPFM and transient SPV techniques, we were able to obtain detailed information on the optoelectronic properties of the sample at the nanometer scale.[23]

A home-built SRSPS spectrometer was employed to study the "actual" photoinduced charge separation on a single $BiVO_4$ crystal at the nanoscale (see Figure S2 for more details). Figure 3a shows KPFM data with a 10 Hz chopped excitation light from a Xenon lamp centered at 395 nm. KPFM with chopped light shows stripes with alternating light and dark signals (Figure 3b). These varying CPD signals are due to the photogenerated charges with chopped light. The stripes are found over the entire particle. The result confirms that the whole particle is irradiated by the chopped light. It is interesting to note that the contrast of the stripes is much more pronounced on the {011} facets. Figure 3c,d show the spatially resolved SPV spectra plotted against phase and amplitude on different facets of a single $BiVO_4$ crystal. For all the spatially resolved SPV spectra, the phase lags between the excitation signal and the obtained CPD signal in Figure 3c are approximately 120° when the incident energy is larger than the band-gap energy (2.4 eV). The featured phase lags are the typical response of n-type semiconductors. All the spectra show an SPV response at photoexcitation energy greater than 2.4 eV, which is super-band excitation SPV. As expected based on the modulated KPFM image, the SPV measured on the side {011} facet (P1, P2) is a much more intense than that on the top {010} facet (P3, P4). The SPV signal on the {011} facet calculated at 3.0 eV is to be 2.5 times more intense than that on the {010} facet. The intense SPV signal on {011} facets coupled with the phase signal indicates that the photoinduced holes for this n-type $BiVO_4$ crystal are being transferred from the bulk to the {011} surface.

The much more intense SPV signal with chopped light on the {011} facet suggests that this facet is preferred for the accumulation of photogenerated holes although the two facets of a single $BiVO_4$ crystal share the same interface with the FTO substrate. The present results suggest that the built-in electric field caused by the surface band bending in the SCR of {011} facet is much stronger than {010} facet. However, as indicated by theoretical calculations in the literatures, the mobility difference of charge carriers between the different facets should also be considered.[24]

Because previous results suggest that the morphology of $BiVO_4$ crystals may influence their photocatalytic performance,[16] $BiVO_4$ crystals (BV02) with preferentially exposed {010} facets were examined by SRSPS. Figure 4a shows the topology image of $BiVO_4$ BV02 crystals. Two spots on the surface of a single $BiVO_4$ crystal, one on the side {011} facet (P1) and another on the top {010} facet (P2), were selected to record the SPV signals, as shown in Figure 4b. The SPV signal on the {011} facet calculated at 3.0 eV is 70 times more intense than that on the {010} facet. This signal is approximately 30 times higher than that of BV01. In addition, it should be noted that there is nearly no SPV signal on the {010} facet of BV02. Obviously, the result suggests that BV02 presents highly anisotropic charge distributions when excited with light, as shown schematically in Figure 4c. The present results further reveal that $BiVO_4$ crystals with preferentially exposed {010} facets show bigger difference in the strength of the built-in electric field between the two facets than is the case for BV01 crystals (shown in Figure 4d).

Single-particle fluorescence microscopy[25] was used to determine whether these photoinduced holes can participate in the photooxidation (Figure S3). The bright fluorescence features on the {011} facets BV01 and BV02 further demonstrated that the

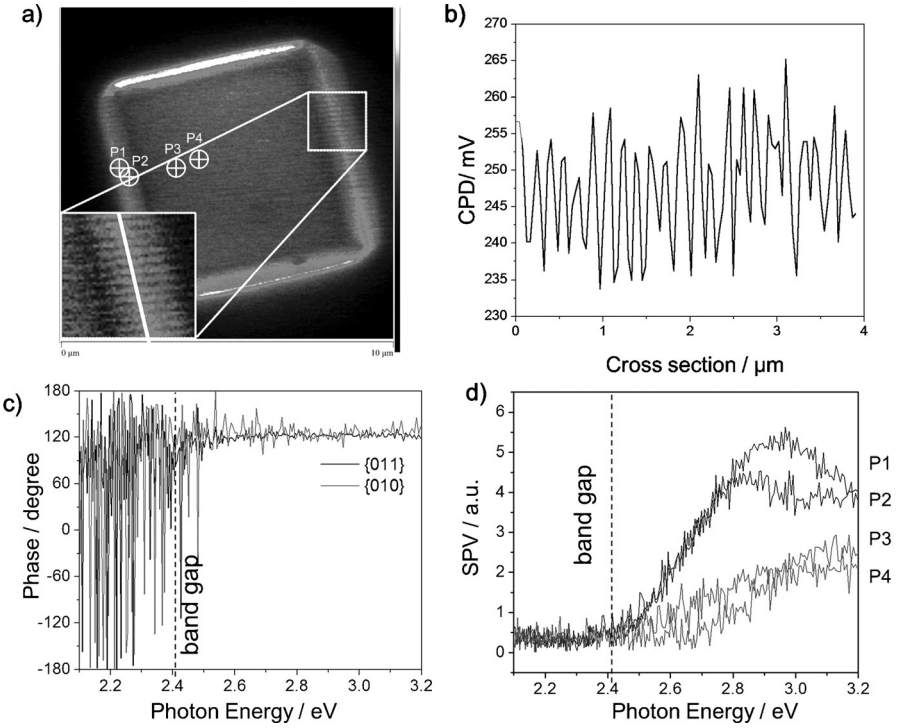

Figure 3. a) KPFM of a single $BiVO_4$ particle (BV01) irradiated with a 10 Hz chopped light from a xenon lamp with scattered light at 395 nm. Inset: selected area. b) Cross-section of the selected area (white square) in (a). c) Spatially resolved SPV phase spectra and d) spatially resolved SPV amplitude spectra at the nanoscale level obtained at different locations of a single $BiVO_4$ crystal, as labeled (a).

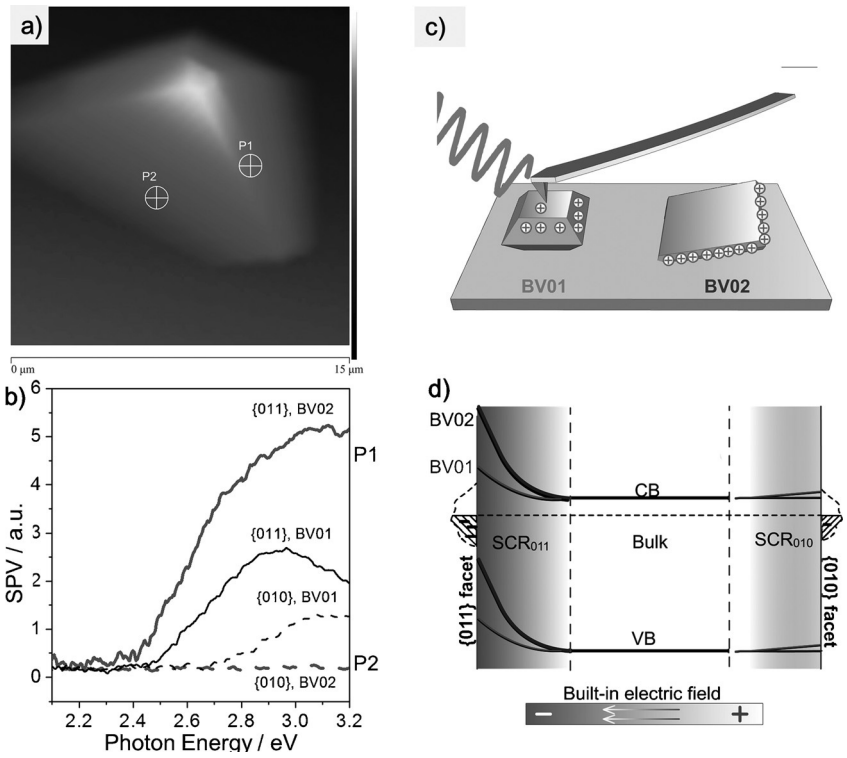

Figure 4. a) Topology image of a single $BiVO_4$ crystal (BV02). b) Spatially resolved SPV spectra obtained at different locations on a single $BiVO_4$ crystal (BV02) as labeled in (a). The thick solid and dashed lines were obtained on the {011} facet (P1) and the {010} facet (P2) as labeled in (a), respectively. The thinner solid and dashed lines were obtained on the {011} and {010} facets of BV01 extracted from Figure 3 d. c) Schematic of the anisotropic charge distributions on a single $BiVO_4$ photocatalyst with different morphologies. d) Schematic of the built-in electric field with relative strength in the SCR of different facets.

anisotropic photogenerated hole transfer observed by SRSPS on the {011} facet can oxidize probe molecules.

In summary, spatially resolved surface photovoltage spectroscopy was employed to obtain direct evidence for anisotropic photoinduced charge transfer between different facets of a single semiconductor crystal. Morphology plays a key role for the anisotropic charge distributions of different facets of single $BiVO_4$ crystals. Highly anisotropic photoinduced hole distribution is observed for single $BiVO_4$ crystals with preferentially exposed {010} facets, and the SPV signal intensity on the {011} facet is 70 times stronger than that on the {010} facet. The influence of the built-in electric field in SCR of different facets on the anisotropic photoinduced charge transfer in a single semiconductor crystal is revealed. The result provides insight into the nature of photogenerated charge separation in a single semiconductor photocatalyst particle and provides an exciting opportunity to optimize the performance of solar energy conversion devices by utilizing the anisotropic charge-transfer properties of single-crystal semiconductors.

Keywords: charge carrier injection · charge separation · crystal engineering · imaging · photocatalysis

How to cite: *Angew. Chem. Int. Ed.* **2015**, *54*, 9111–9114
Angew. Chem. **2015**, *127*, 9239–9242

Received: May 6, 2015
Published online: July 3, 2015

[1] A. Marchioro, J. Teuscher, D. Friedrich, M. Kunst, R. van de Krol, T. Moehl, M. Grätzel, J. E. Moser, *Nat. Photonics* **2014**, *8*, 250–255.
[2] S. C. Warren, K. Voitchovsky, H. Dotan, C. M. Leroy, M. Cornuz, F. Stellacci, C. Hebert, A. Rothschild, M. Grätzel, *Nat. Mater.* **2013**, *12*, 842–849.
[3] Y. Terada, S. Yoshida, O. Takeuchi, H. Shigekawa, *Nat. Photonics* **2010**, *4*, 869–874.
[4] D. C. Coffey, D. S. Ginger, *Nat. Mater.* **2006**, *5*, 735–740.
[5] S. U. Nanayakkara, G. Cohen, C. S. Jiang, M. J. Romero, K. Maturova, M. Al-Jassim, J. van de Lagemaatt, Y. Rosenwaks, J. M. Luther, *Nano Lett.* **2013**, *13*, 1278–1284.
[6] G. Liu, J. C. Yu, G. Q. Lu, H. M. Cheng, *Chem. Commun.* **2011**, *47*, 6763–6783.
[7] A. Vittadini, A. Selloni, F. P. Rotzinger, M. Grätzel, *Phys. Rev. Lett.* **1998**, *81*, 2954–2957.
[8] M. Lazzeri, A. Vittadini, A. Selloni, *Phys. Rev. B* **2001**, *63*, 155409.
[9] G. S. Herman, M. R. Sievers, Y. Gao, *Phys. Rev. Lett.* **2000**, *84*, 3354–3357.
[10] X. Q. Gong, A. Selloni, *J. Phys. Chem. B* **2005**, *109*, 19560–19562.
[11] H. G. Yang, C. H. Sun, S. Z. Qiao, J. Zou, G. Liu, S. C. Smith, H. M. Cheng, G. Q. Lu, *Nature* **2008**, *453*, 638–641.
[12] T. Ohno, K. Sarukawa, M. Matsumura, *New J. Chem.* **2002**, *26*, 1167–1170.
[13] T. Tachikawa, S. Yamashita, T. Majima, *J. Am. Chem. Soc.* **2011**, *133*, 7197–7204.
[14] R. G. Li, F. X. Zhang, D. G. Wang, J. X. Yang, M. R. Li, J. Zhu, X. Zhou, H. X. Han, C. Li, *Nat. Commun.* **2013**, *4*, 1432.
[15] K. Wenderich, A. Klaassen, I. Siretanu, F. Mugele, G. Mul, *Angew. Chem. Int. Ed.* **2014**, *53*, 12476–12479; *Angew. Chem.* **2014**, *126*, 12684–12687.
[16] D. E. Wang, H. F. Jiang, X. Zong, Q. A. Xu, Y. Ma, G. L. Li, C. Li, *Chem. Eur. J.* **2011**, *17*, 1275–1282.
[17] a) S. Hudlet, M. Saintjean, B. Roulet, J. Berger, C. Guthmann, *J. Appl. Phys.* **1995**, *77*, 3308–3314; b) W. Melitz, J. Shen, A. C. Kummel, S. Lee, *Surf. Sci. Rep.* **2011**, *66*, 1–27.
[18] S. Sadewasser, T. Glatzel, M. Rusu, A. Jager-Waldau, M. C. Lux-Steiner, *Appl. Phys. Lett.* **2002**, *80*, 2979–2981.
[19] C. Y. Chao, Z. H. Ren, Y. H. Zhu, Z. Xiao, Z. Y. Liu, G. Xu, J. Q. Mai, X. Li, G. Shen, G. R. Han, *Angew. Chem. Int. Ed.* **2012**, *51*, 9283–9287; *Angew. Chem.* **2012**, *124*, 9417–9421.
[20] L. Kronik, Y. Shapira, *Surf. Sci. Rep.* **1999**, *37*, 1–206.
[21] A. Winnerl, R. N. Pereira, M. Stutzmann, *Phys. Rev. B* **2015**, *91*, 075316.
[22] A. Morawski, M. M. G. Slusarczuk, J. Lagowski, H. C. Gatos, *Surf. Sci.* **1977**, *69*, 53–61.
[23] F. Streicher, S. Sadewasser, M. C. Lux-Steiner, *Rev. Sci. Instrum.* **2009**, *80*, 013907.
[24] a) D. J. Martin, N. Umezawa, X. W. Chen, J. H. Ye, J. W. Tang, *Energy Environ. Sci.* **2013**, *6*, 3380–3386; b) Z. Y. Zhao, Z. S. Li, Z. G. Zou, *Phys. Chem. Chem. Phys.* **2009**, *13*, 4746–4753.
[25] T. Tachikawa, S. Yamashita, T. Majima, *Angew. Chem. Int. Ed.* **2010**, *49*, 432–435; *Angew. Chem.* **2010**, *122*, 442–445.